

Dalton Transactions

Accepted Manuscript



This is an *Accepted Manuscript*, which has been through the Royal Society of Chemistry peer review process and has been accepted for publication.

Accepted Manuscripts are published online shortly after acceptance, before technical editing, formatting and proof reading. Using this free service, authors can make their results available to the community, in citable form, before we publish the edited article. We will replace this *Accepted Manuscript* with the edited and formatted *Advance Article* as soon as it is available.

You can find more information about *Accepted Manuscripts* in the [Information for Authors](#).

Please note that technical editing may introduce minor changes to the text and/or graphics, which may alter content. The journal's standard [Terms & Conditions](#) and the [Ethical guidelines](#) still apply. In no event shall the Royal Society of Chemistry be held responsible for any errors or omissions in this *Accepted Manuscript* or any consequences arising from the use of any information it contains.

ARTICLE

Ferrocenylmethylation reactions with a phosphinoferrocene betaine

Cite this: DOI: 10.1039/x0xx00000x

Martin Zábanský,^a Ivana Císařová,^a and Petr Štěpnička^{a*}Received 00th January 2015,
Accepted 00th January 2015

DOI: 10.1039/x0xx00000x

www.rsc.org/

A phosphinoferrocene betaine, *N*-{[(1'-diphenylphosphino)ferrocenyl]methyl}-*N,N*-dimethyl-3-sulfo-1-propanaminium, inner salt, Ph₂PfcCH₂NMe₂(CH₂)₃SO₃ (**2**; fc = ferrocene-1,1'-diyl), was prepared by alkylation of Ph₂PfcCH₂NMe₂ (**1**) with 1,3-propanesultone, and was studied as a ferrocenylmethylation agent. The treatment of **2** with NaOH in hot water-dimethyl sulfoxide produced phosphinoalcohol Ph₂PfcCH₂OH (**3**) in a 64% yield, whereas a similar reaction with MeONa in dimethylsulfoxide-methanol furnished the corresponding ether, Ph₂PfcCH₂OMe (**4**), in a 47% yield. In subsequent experiments, betaine **2** was employed in the synthesis of phosphinoferrocene sulfones, Ph₂PfcCH₂SO₂R, where R = Me (**6a**), Ph (**6b**), and 4-tolyl (**6c**). Compounds **6a-c** and some by-products of the ferrocenylmethylation reactions, namely alcohol **3**, 1'-(diphenylphosphino)-1-methylferrocene (**5**), and 1'-[[diphenyl(2,4-cyclopentadien-1-ylidene)phosphoranyl]methyl]-1'-(diphenylphosphino)ferrocene (**7**) were structurally characterised. Reactions of **6a** as the representative with ZnX₂/NaX (X = Br and I) afforded unique coordination polymers [ZnNaX₃(**6a**)(CH₃OH)]_n featuring tetrahedral Zn(II) and octahedral Na(I) centres bridged by halide ions, solvating methanol and the sulfone ligands. The reaction of **6a** with ZnBr₂/KBr produced an analogous product, [ZnKBr₃(**6a**)(CH₃OH)]_n, while that with ZnBr₂/LiBr furnished a different, pseudodimeric complex [Zn₂Li₂Br₆(**6a**)₂(CH₃OH)₄(H₂O)]·CH₃OH, featuring tetrahedrally coordinated Zn(II) and Li(I) centres bridged by **6a**. Reactions of **6a** with ZnBr₂/MBr (M = Rb, Cs) and NaCl/ZnCl₂ did not yield similar products because of an easy precipitation (low solubility) of the respective alkali metal halides.

Introduction

Shortly after the discovery of ferrocene¹ and the elucidation of its real structure² in the early 1950s, ferrocenylmethylation was recognised as a powerful method for the preparation of various ferrocene derivatives.³ This reaction typically utilises stable starting materials capable of serving as precursors of the stabilised ferrocenylmethyl cation,⁴ which is allowed to react with nucleophiles (Nu) to afford derivatives of the type FcCH₂Nu (Fc = ferrocenyl). The most often employed ferrocenylmethylation reagents are undoubtedly FcCH₂NMe₂ and [FcCH₂NMe₃]I, with which the reaction was developed, though other compounds, e.g., [FcCH₂PPh₃]I or FcCH₂OH (the latter in combination with an acid), have also found practical applications.³

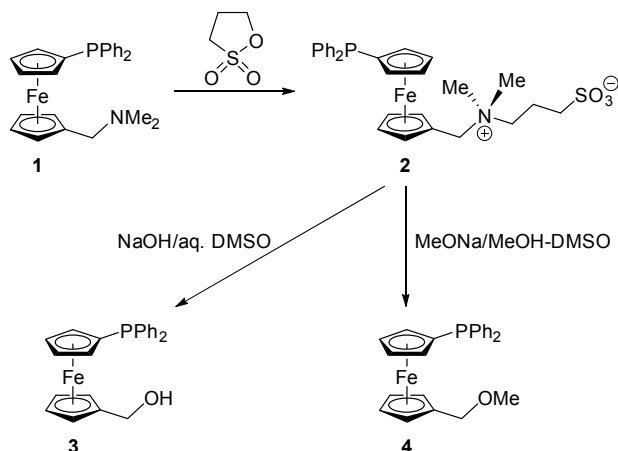
In the synthesis of phosphinoferrocene donors,⁵ ferrocenylmethylation reactions have been applied only rarely because of competitive reactions affecting the phosphine moieties (alkylation).⁶ Therefore, the [1'-(diphenylphosphino)ferrocene-1-yl]methyl derivatives have typically been synthesised either indirectly (e.g., via late-stage lithiation/phosphinylation⁷) or from P-protected building blocks, such as Ph₂P(S)fcCH₂OH⁸ or the borane adduct Ph₂PfcCH₂OH·BH₃.⁹

In view of our recent work focusing on the preparation and coordination properties of 1'-(diphenylphosphino)-1'-[[dimethylamino]methyl]ferrocene (**1**)^{10,11} and other 1'-functionalised phosphinoferrocene derivatives possessing an inserted methylene group,^{9,12} we wanted to extend the hitherto unexplored synthetic chemistry of the former compound, which led us to attempt at the preparation of ammonium salts derived from **1** and study their prospective synthetic applications. In this contribution, we describe the selective synthesis and structural characterisation of phosphinoferrocene betaine Ph₂PfcCH₂N⁺Me₂(CH₂)₃SO₃⁻ (**2**; fc = ferrocene-1,1'-diyl) and its utilisation in the preparation of the known and some new 1'-functionalised phosphinoferrocene donors such as 1'-[[diphenylphosphino)ferrocenyl]methyl sulfones Ph₂PfcCH₂SO₂R. Furthermore, we report on the reactions of the representative ligand, Ph₂PfcCH₂SO₂Me, with zinc(II) and alkali metal halides, leading to structurally unique mixed-metal coordination polymers.

Results and Discussion

Synthesis of betaine **2** and initial reaction tests

Betaine **2** was synthesised similarly to its non-phosphinylated analogue (Scheme 1)¹³ by the reaction of phosphinoamine **1**¹⁰ with 1,3-propanesultone (1,2-oxathiolane-2,2-dioxide) in dry benzene. The compound was isolated by column chromatography, resulting in an air-stable orange solid in an 81% yield (at 10 mmol scale).¹⁴ Crystallisation from methanol-tetrahydrofuran-diethyl ether afforded the stoichiometric solvate **2**·CH₃OH, which was structurally characterised by single-crystal X-ray diffraction analysis (*vide infra*).



Scheme 1. Synthesis and model reactions of betaine **2**.

The ¹H and ¹³C NMR spectra of **2** combine the signals due to the phosphinoferrocenyl moiety with those of the NMe₂ group and the propane-1,3-diyl bridge. The ³¹P NMR resonance is observed at δ_p −18.1 ppm, suggesting that the phosphine moiety remained intact. In its IR spectrum, betaine **2** shows strong signals attributable to the vibrations of the terminal sulfonate moiety (ν_s 1037 cm^{−1} and ν_{as} 1189 cm^{−1}), whereas the electrospray ionisation (ESI) mass spectrum reveals signals of the pseudomolecular ions [M + X]⁺, where M = H, Na, and K, and of the characteristic fragment¹⁵ ions due to the substituted ferrocenylmethyl cation [Ph₂PfcCH₂]⁺ at *m/z* 383.

The possible synthetic applications of betaine **2** were first examined by its conversion into the known alcohol **3**^{12a} and the corresponding methyl ether **4**⁹ via reactions with the respective nucleophiles (Scheme 1). These ferrocenylmethylation reactions were carried out similarly to the literature^{13,16} but carefully optimised. For solubility reasons, dimethyl sulfoxide was chosen as the solvent, and the reactions were performed at temperatures above 100 °C since lower reaction temperatures markedly reduced the yield of the substitution product (N.B. unreacted **2** could be recovered from the reaction mixture in such cases). The reaction time was kept at minimum (typically 1 h) in order to prevent decomposition and oxidation of the phosphine moiety.

For the preparation of alcohol **3**, the best reaction conditions were found to consist of refluxing the solution of betaine **2** in a mixture of DMSO and 2 M aqueous NaOH (1:1; the concentration of NaOH in the resulting solution was 1 M) for 1 h. The product **3** was isolated by extraction and purified by

column chromatography, resulting in a 64% yield (at 2 mmol scale). A small amount of a less polar side-product was also isolated, being identified as 1'-(diphenylphosphino)-1-methylferrocene, Ph₂PfcMe (**5**; typically ca. 5%). This rather unexpected product probably results via “quenching” of the intermediate cation Ph₂PfcCH₂⁺ upon attack of other C-H bonds (acid-base equilibria) rather than by interaction with any proton source in the reaction system.

The etherification reaction was similarly performed in a mixture of dimethyl sulfoxide and methanolic MeONa (1 M MeONa in the reaction system) at lower temperatures (but still under reflux conditions) for 2 h, affording phosphinoether **4** in a 47% isolated yield.

The crystal structures of **2**·CH₃OH and **5**

The solvate **2**·CH₃OH, isolated after crystallisation by liquid-phase diffusion of tetrahydrofuran and diethyl ether into a solution of the betaine in methanol, crystallises with the symmetry of the triclinic space group *P*−1. Its structure is presented in Figure 1, and the relevant geometric data are summarised in Table 1.

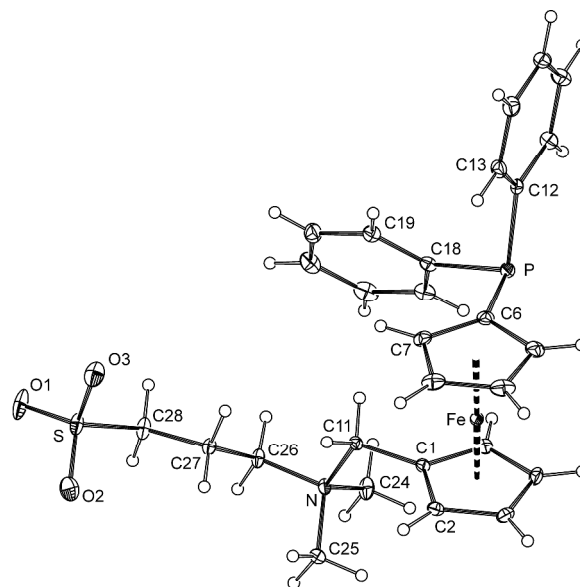


Figure 1. PLATON plot of the phosphinobetaine molecule in the structure of **2**·CH₃OH showing the atom-labelling scheme and displacement ellipsoids at a 30% probability level.

The ferrocene unit in the structure of **2** shows similar Fe-C distances (2.019(1)–2.051(1) Å) and, accordingly, practically negligible tilting (the dihedral angle of the least-squares planes of the cyclopentadienyl ring is 1.40(8)°). The substituents attached to the ferrocene moiety adopt a nearly ideal synclinal eclipsed conformation, as evidenced by the torsion angle C1–Cg1–Cg2–C6 of −73.49(9)° (cf. the ideal value of 72°).

The carbons surrounding the positively charged nitrogen atom in **2** constitute a regular tetrahedral environment, with the C-N distances and associated bond angles (C-N-C) in the range of 1.497(2)–1.525(2) Å and 106.9(1)–111.0(1)°, respectively. The environment of the sulfur atom is somewhat distorted,

presumably because of the different sizes of the bonded atoms and, also, a repulsion of the oxygen atoms ($S-C > S=O$ and $O=S=O > C-S=O$; see parameters in Table 1).

Table 1. Selected interatomic distances and angles for **2**·CH₃OH (in Å and deg).^a

Distances		Angles	
S-O1	1.463(1)	C6-P-C12	102.25(6)
S-O2	1.450(1)	C6-P-C18	101.92(6)
S-O3	1.454(1)	C12-P-C18	102.45(6)
S-C28	1.777(2)	O1-S-O2	112.85(7)
N-C11	1.525(2)	O1-S-O3	113.21(7)
N-C24	1.499(2)	O2-S-O3	113.00(7)
N-C25	1.497(2)	C28-S-O1	103.67(7)
N-C26	1.518(2)	C28-S-O2	106.38(7)
P-C6	1.811(1)	C28-S-O3	106.84(7)
P-C12	1.834(1)	C1-C11-N-C26	-177.8(1)
P-C18	1.837(1)	C11-N-C26-C27	-54.8(1)
C1-C11	1.489(2)	N-C26-C27-C28	-172.0(1)
C1S-O1S	1.412(2)	C26-C27-C28-S	171.39(9)

^a Note: parameters pertaining to the ferrocene moiety as well as the N-C-N angles are discussed in the main text.

The individual molecules constituting the crystals of **2**·CH₃OH assemble into dimers of inversion-related molecules through charge-supported hydrogen bonds between two oxygen atoms of the negatively charged sulfonate group and the CH₃ hydrogens polarised by the positively charged nitrogen (Figure 2). The solvating methanol forms an O-H...O hydrogen bond with the remaining sulfonate oxygen. Additional C-H...O interactions further interconnect the (**2**)₂(CH₃OH)₂ units into columnar stacks oriented along the crystallographic *a*-axis.

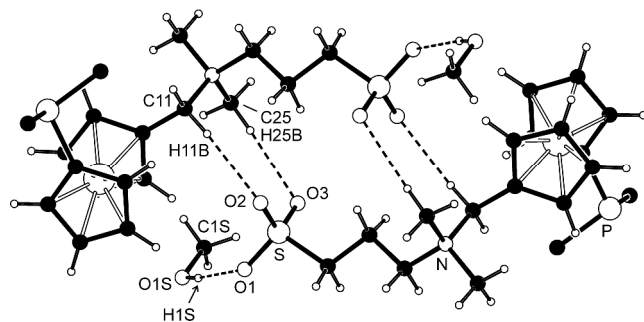


Figure 2. View of the hydrogen bonded dimers in the structure of **2**·CH₃OH. For clarity, only the pivotal atoms of the phenyl rings are shown. The hydrogen bond parameters are as follows: C11-H11B...O2¹: C11...O2 = 3.417(2) Å, angle at H11 = 166°; C25-H25B...O3¹: C25...O3 = 3.396(2) Å, angle at H25B = 167°; O1S-H1S...O1¹: O1S...O1 = 2.719(2) Å, angle at H1S = 172°; i. (1-x, 1-y, 2-z).

The solid-state structure of **5** (Figure 3) resembles that of the corresponding borane adduct **5**·BH₃.⁹ Whereas the C1-C11 bond lengths (1.497(2) Å) in both compounds are practically identical (within the three-sigma level), the P-C bonds in **5** (P-C6 1.810(2), P-C12 1.841(2), and P-C18 1.834(2) Å) are slightly but statistically significantly longer (by ca. 0.02 Å) than those in the mentioned reference compound, reflecting the electronic changes associated with the adduct formation ($R_3P \rightarrow BH_3$). The Fe-C distances in the molecule of **5** span a narrow range of 2.037(1)-2.051(2) Å, which is in turn reflected in an insignificant tilting of the cyclopentadienyl rings (the tilt

angle is as low as 1.1(1)°). As indicated by the torsion angle C1-Cg1-Cg2-C6 of -77.8(1)°, the ferrocene unit has a synclinal eclipsed conformation, which is also similar to that of the aforementioned borane adduct.

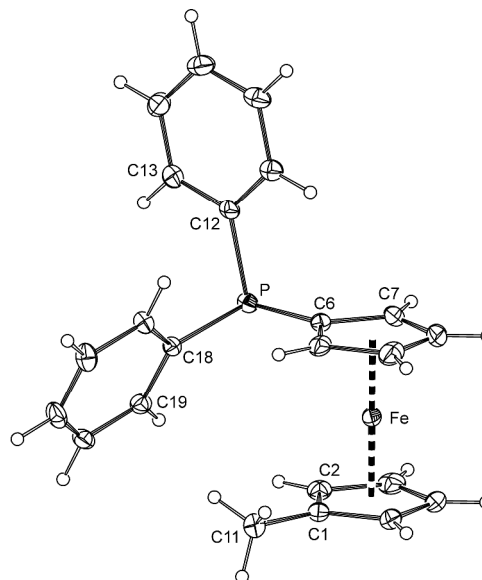
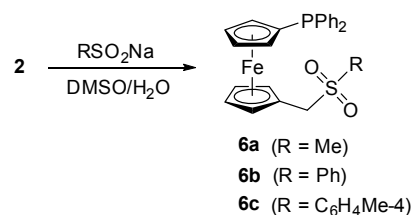


Figure 3. PLATON plot of the molecular structure of **5** showing 30% displacement ellipsoids.

Synthesis and characterisation of phosphine-sulfones **6**

Aiming at the preparation of *new* phosphinoferrocene ligands via ferrocenylmethylation, betaine **2** was subsequently reacted with sodium sulfonates to give the respective phosphinoferrocene sulfones **6** (Scheme 2). The reactions were performed with an excess of the sulfinate salts (**2**:RSO₂Na = 1:2.5) in refluxing DMSO-water for 2 h, similarly to the synthesis of ferrocenylmethyl sulfones FcCH₂SOR from simple ferrocenylmethylation agents.^{17,13}

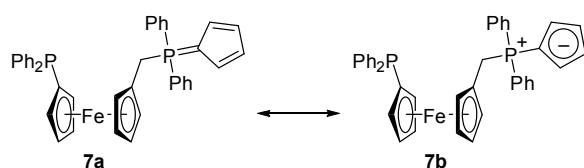


Scheme 2. Preparation of phosphinoferrocenyl sulfones **6**.

The yields of the sulfones after chromatographic purification were ca. 30% for **6a** and approximately 50% for the compounds bearing the aromatic substituents (**6b** and **6c**), which are less than in the reactions leading to FcSO₂R. Therefore, we sought for other reaction products to gain more detailed information regarding the course of these particular ferrocenylmethylation reactions.

In the case of the reaction of betaine **2** with MeSO₂Na, a careful chromatographic purification of the reaction mixture led to the isolation of alcohol **3** (2%) and phosphorane **7** (Scheme 3; 12%). Together with **6a**, compounds **3** and **7** account for

nearly 45% of the starting material. The reactions leading to aryl sulfones **6b** and **6c** are more selective (isolated yields: ca. 50%) but afford identical by-products (isolated yields of **3** and **7** are ca. 3% and 10-15%, respectively). Apparently, the cation $\text{Ph}_2\text{PfcCH}_2^+$ generated *in situ* from **2** enters into reactions with all other available nucleophiles, including OH^- or phosphines. Interaction with the latter provides cationic products (i.e., phosphonium salts arising from “self-alkylation” of the parent **2** with $\text{Ph}_2\text{PfcCH}_2^+$) and, consequently, also their decomposition products such as **7**. The fact that no **7** could be detected in the reaction mixtures obtained after treatment of **2** with NaOH and NaOMe (*vide supra*) can well reflect the higher relative amounts of these nucleophilic reagents, that suppress the competing reactions with other nucleophiles. Attempts to isolate the anticipated cationic (and hence more polar) side products or to recover unreacted **2** during the course of chromatographic purification of crude sulfones **6** failed.



Scheme 3. Canonical forms of compound **7**.

The formulation of **6a-c** and **7** was inferred from NMR and IR spectra, ESI mass spectra, and elemental analysis and was unequivocally confirmed by single-crystal X-ray diffraction. The NMR spectra of sulfones **6** comprise the signals due to the (diphenylphosphino)ferrocenyl unit and its attached methylene linker (CH_2 : $\delta_{\text{H}}/\delta_{\text{C}}$ 3.59/56.65 for **6a**, and ca. 3.68/58.3 for **6b** and **6c**). The signals of the sulfone substituents, as well as the ^{31}P NMR resonances ($\delta_{\text{P}} \approx -17$ ppm), are observed in the usual ranges. The IR spectra of the sulfones display the characteristic strong bands of the sulfone moieties centred at approximately 1310 (ν_{as}) and 1145 cm^{-1} (ν_{s}).^{17a}

The ^1H and ^{13}C NMR spectra of the by-product **7** contain signals of the 1,1'-disubstituted ferrocene moiety and two sets of resonances of the non-equivalent PPh_2 groups, which is also reflected in the ^{31}P NMR spectrum showing two singlets at $\delta_{\text{P}} -16.9$ and 10.1. The presence of the cyclopentadienylidene unit¹⁸ in **7** is manifested by a pair of multiplets at δ_{H} 6.12 and 6.40 and a pair of doublets at δ_{C} 113.92 and 115.83 in the ^1H and ^{13}C NMR spectra, respectively. The ^{13}C NMR signal due to C_{ipso} in the $\text{P}=\text{C}_5\text{H}_4$ moiety is observed at δ_{C} 78.21 as a phosphorus-coupled doublet ($^1J_{\text{PC}} = 110$ Hz). The signals of the connecting methylene group are found at δ_{H} 3.59 (doublet with $^2J_{\text{PH}} = 12.7$ Hz) and δ_{C} 30.01 (dd, $^1J_{\text{PC}} = 53$, $J_{\text{PC}} = 1$ Hz).

Crystallisation of **6a** from ethyl acetate-hexane provided crystals of a triclinic modification (denoted as **6a**). Crystals of another polymorph, **6a'**, were serendipitously isolated during an attempted preparation of Zn(II) complexes, i.e., upon crystallization of a **6a**/ZnBr₂ mixture from methanol-diethyl ether (*vide infra*). The polymorphs differ by the symmetry of the crystal lattice (**6a**: triclinic, $P\bar{1}$; **6a'**: monoclinic, $P2_1/c$)

and by the overall conformation of the molecules constituting their crystals (Figure 4 and Table 2).

Thus, whereas the molecular structures of the two polymorphs are expectedly very similar in terms of interatomic distances and angles, they differ in the mutual orientation of the substituted cyclopentadienyl rings, which are nearly synclinal eclipsed in **6a** and exactly halfway between anticlinal eclipsed and antiperiplanar staggered in **6a'** (compare the C1-Cg1-Cg2-C6 angles in Table 1).¹⁹ Another, less pronounced difference can be observed in the orientation of the PPh_2 units resulting from different rotations along the pivotal C6-P bond and from the tilting of the phenyl rings.

The geometry of the (methylsulfonyl)methyl moiety in **6a** and **6a'** compares well with that of, e.g., phenyl methyl sulfone, 4-methoxyphenyl methyl sulfone,²⁰ and (benzylsulfonyl)methanol.²¹ Similar to these compounds, the O1-S-O2 angle is the most opened and the C11-S-C24 angle is the most acute among the bond angles around the sulfur atoms in **6a** and **6a'**, most likely due to an electrostatic repulsion of the electronegative oxygen atoms.

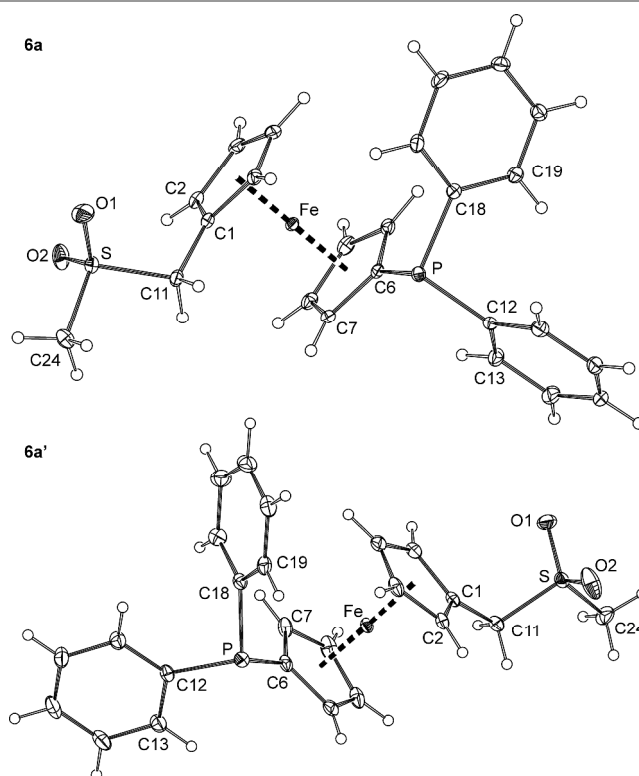


Figure 4. PLATON plots of the molecular structures of the triclinic (top; **6a**) and monoclinic (bottom; **6a'**) polymorphs of 1'-(diphenylphosphino)-1-[(methylsulfonyl)methyl]ferrocene. The displacement ellipsoids enclose the 30% probability level.

The main difference between the molecular structures of sulfones **6b** and **6c** (Figure 5 and Table 2) can also be found in the conformation of the 1,1'-disubstituted ferrocene unit, which is intermediate between anticlinal staggered and anticlinal eclipsed for **6b** and synclinal eclipsed for **6c**. In both cases, the $\text{CH}_2\text{SO}_2\text{Ar}$ (Ar is an aryl) pendants extend away from the

ferrocene core but adopt different orientations as indicated by the torsion angles C1-C11-S-C24 (see Table 2) and the dihedral angles of the C(1-5) and C(24-29) ring planes of 45.93(8)° and 33.5(1)° for **6b** and **6c**, respectively. On the other hand, the compounds comprise regular ferrocene moieties (tilt angles below ca. 3°) and show similar individual interatomic distances and angles that do not depart substantially from those of **6a/6a'** and benzylsulfones of the type ArCH₂SO₂Ar (Ar = an aryl).²²

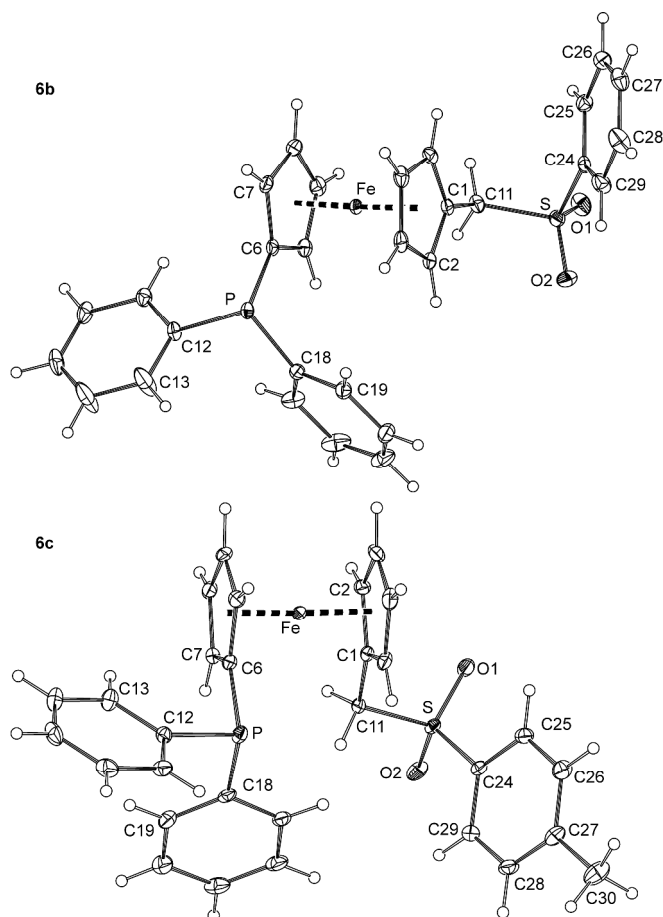


Figure 5. PLATON plots of the molecular structure of the phosphinoferrocene sulfones **6b** and **6c** at the 30% probability level.

The ferrocene cyclopentadienyls in the structure of by-product **7** (Figure 6) are tilted by 2.6(1)° and assume a conformation near synclinal eclipsed, as evidenced by the C1-Cg1-Cg2-C6 torsion angle of 79.3(1)°. The individual Fe-C distances are in the range of 2.026(2)–2.050(2) Å. The cyclopentadienylidene substituent at the phosphorus P2 exhibits only moderate bond alternation (C31–C32 1.425(3), C32–C33 1.382(3), C33–C34 1.406(3), C34–C35 1.382(3), and C35–C31 1.414(3) Å). Its pivotal P2–C31 bond (1.722(2) Å) is of similar length to those in MePh₂P=C₅R₄ (R = H: 1.728(2) and 1.727(2) Å;¹⁸ R = Me: 1.720(2) and 1.717(2) Å²³). As such, it is shorter than the P1–C6 bond in **7** (1.811(2) Å) and the P⁺–C₅H₄ bond in [Fe(η⁵-C₅H₄P⁺Ph₂Me){η⁵-C₅H₄Cr(CO)₆}] (1.769(5) Å)²⁴ but longer than the P=CH₂ bond in the archetypal phosphorane Ph₃P=CH₂ (1.662(8) and 1.659(8) Å).²⁵ These features suggest

compound **7** to possess an intermediate structure between two extreme canonical forms, *viz* cyclopenta-2,4-dien-1-ylidene phosphorane (**7a**) and zwitterionic phosphonium cyclopentadienide (**7b**), as depicted in Scheme 3. It is also noteworthy that the P–Ph bonds are significantly longer for P1 (P1–C12 1.839(2), P1–C18 1.841(2) Å) than for P2 (P2–C36 1.801(2), P2–C42 1.810(2) Å), which bears a partial positive charge, most likely due to an electron density transfer from the aromatic rings to the partly positively charged P2. In contrast, the length of the P2–C11 bond (1.817(2) Å) compares well with to that of the similar bond in the phosphonium salt [FcPPh₂(CH₂Ph)]Cl (1.819(3) Å).²⁶

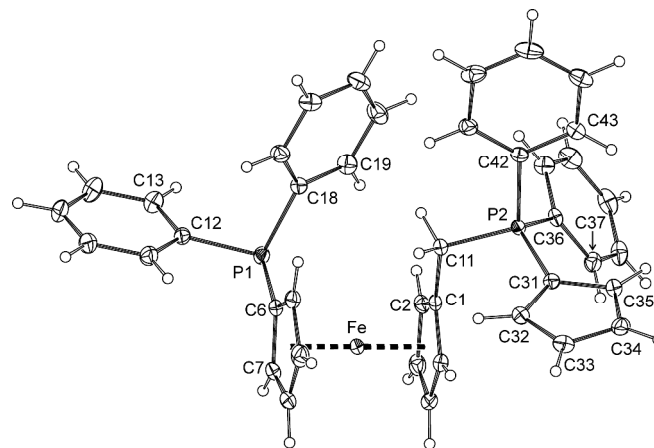


Figure 6. PLATON plot of the molecular structure of **7** (30% displacement ellipsoids).

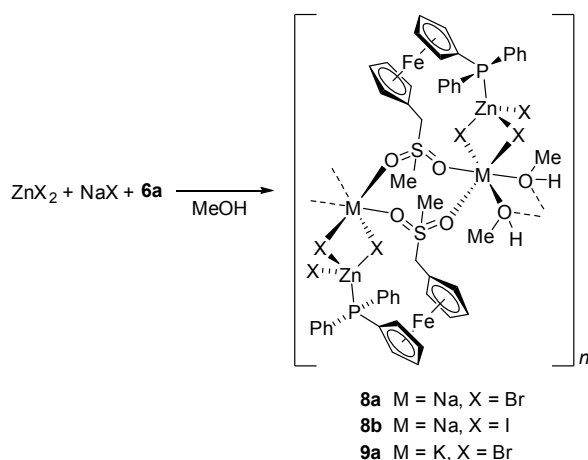
Preparation and structure of mixed-cation complexes with **6a**

Coordination preferences of the newly prepared phosphinoferrocene sulfones were studied in reactions of **6a** as the model representative, with zinc(II) halides. These salts were chosen mainly due to the position of the Zn(II) ion at the borderline between hard and soft metal ions²⁷ and due to its closed (d¹⁰) coordination sphere, which makes it structurally variable because of the absence of crystal-field stabilisation.²⁸

To our disappointment, repeated experiments aiming at the preparation of defined products by co-crystallisation of zinc(II) halides with **6a** were unsuccessful. In one case, the crystallisation of a ZnBr₂–**6a** mixture in methanol/diethyl ether provided crystals of monoclinic **6a'**. Eventually, the attempted preparation of a Zn(II) complex by reacting ZnBr₂ and **6a** at a 1:1 molar ratio in methanol-chloroform, followed by evaporation and crystallisation from CHCl₃/methyl *tert*-butyl ether, yielded a few crystals of **8b**, which were used directly for X-ray structure determination.²⁹ The intriguing structure of this rather unexpected product (*vide infra*) led us to study the formation of such complexes systematically by changing the halide in ZnX₂/NaX (NaCl – NaBr – NaI) and then also the alkali metal cation in ZnBr₂/MBr (M = Li, Na, K, Rb, and Cs).

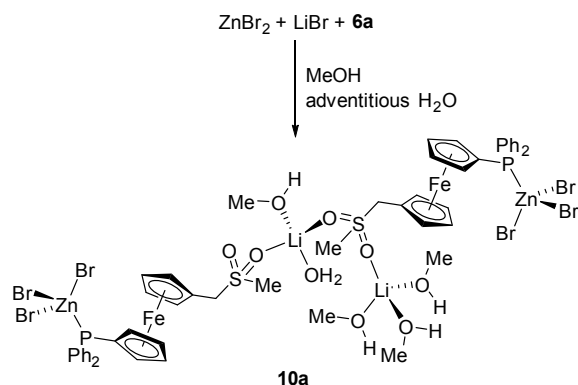
Attempts to isolate any mixed-cation compound from the **6a**/ZnCl₂/NaCl system failed, presumably because of the ionic nature of NaCl, which limits its solubility in organic solvents. The experiments furnished only crystals of uncoordinated **6a**.

On the other hand, the reactions of **6a** with NaX/ZnX₂, where X = Br and I (all in equimolar amounts), in methanol followed by crystallisation upon layering the reaction mixture with methyl *tert*-butyl ether produced the respective coordination polymers **8a** (X = Br) and **8b** (X = I) as orange, nicely crystalline, and air-stable solids in good yields (Scheme 4).



Scheme 4. Preparation of the mixed-metal complexes **8a**, **8b** and **9a**.

The reactions of **6a** with ZnBr₂ with other alkali metal bromides were performed similarly to the preparation of the mentioned Na-Zn complexes but in solvent mixtures with an optimised chloroform/methanol ratio to ensure sufficient solubility of the alkali metal halide and not suppress separation of the product after the addition of methyl *tert*-butyl ether.³⁰ Attempted reactions with RbBr and CsBr did not afford any M-Zn complex because these salts separated from the reaction mixture, whereas the analogous reaction of **6a** with ZnBr₂ and KBr produced K-Zn complex **9a** (Scheme 4), which adopts the structure of its sodium congener. In contrast, the reaction **6a** with ZnBr₂ and LiBr produced a Zn-Li complex [Zn₂Li₂Br₆(**6a**)₂(CH₃OH)₄(H₂O)]·CH₃OH (**10a**·CH₃OH). In its structure, the phosphinoferrocene ligands coordinate the terminal ZnBr₃ units via their phosphine groups (similarly to the Na-Zn and K-Zn complexes) and further bind solvated Li⁺ ions via the sulfone oxygens to form a discrete pseudodimeric assembly (Scheme 5).³¹



Scheme 5. Preparation of the Li-Zn complex **10a**.

The M-Zn complexes (M = alkali metal cation) disintegrate upon dissolving in donor solvents. This was evidenced by the ¹H and ³¹P{¹H} NMR spectra recorded for solutions of crystalline **8a** in CD₃OD that reveal the exclusive presence of uncoordinated **6a** in solution (δ_P −16.3 ppm) and also by the ESI mass spectra showing only signals due to **6a** and its fragments (see Experimental). The same applies to the elusive **6a**-ZnBr₂ complexes (intermediates) as similar features have been observed in the NMR and ESI MS spectra of a residue obtained by evaporation of a 1:1 mixture of **6a**-ZnBr₂. Hence, the characterisation of the mixed-metal complexes had to be confined to solid-state techniques. Unfortunately, the IR spectra were of little diagnostic value because of their relative complexity (see ESI, Figure S1) and only marginal shifts of the diagnostic bands upon coordination (e.g., the bands due to the sulfone moiety as compared to uncoordinated **6a**). Nonetheless, the IR spectra of **8a**, **8b** and **9a** were very similar, suggesting analogous structures for these compounds, and displayed additional broad bands attributable to ν_{OH} vibrations at ca. 3470-3490 cm⁻¹, attributable to the “solvating” methanol. Nonetheless, unequivocal structural information was gained from single-crystal X-ray diffraction analysis.

Compounds **8a** and **8b** are essentially isostructural, and the minor differences in the lattice parameters and atomic coordinates are associated with the different sizes of the halide anions. Compound **9a** has also practically the same structure, albeit described by different cell parameters because even a small variation in the cell angles near 90° as in this particular case can result in another reduced triclinic cell setting.³² The structure of **8a** is depicted in Figure 7, and the displacement ellipsoid plots for all three compounds are presented in the ESI (Figures S2-S4). Pertinent geometric parameters are given in Table 3.

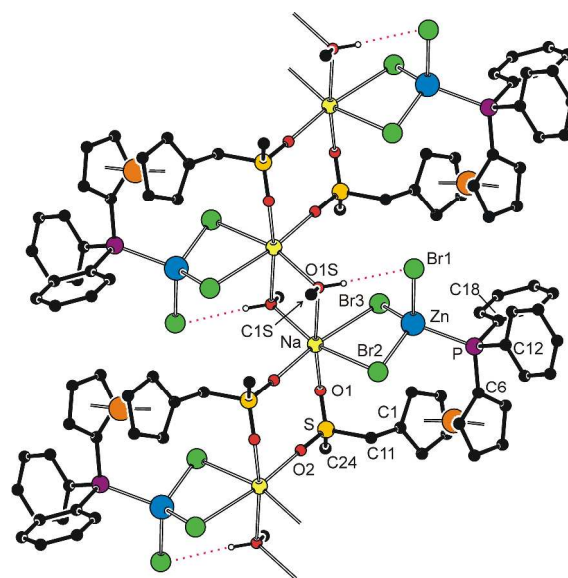


Figure 7. Section of the infinite coordination chain in the structure of **8a** (for a conventional displacement ellipsoid plot, see the ESI). For clarity, the CH hydrogens are omitted, and the CH₃OH...Br hydrogen bond is indicated by a red

dotted line (O1S...Br1 = 3.599(2) Å; the corresponding distance in the structures of **8b** and **9a** are as follows: **8b**, O1S...I1 = 3.828(3) Å; **9a**, O1S...Br1 = 3.540(2) Å).

The compounds are one-dimensional coordination polymers in which the $ZnX_3(6a-\kappa P)$ units coordinate the Na(I) ions via two halide ions (bridging X2 and X3) and the sulfone oxygen O1. The coordination sphere of the Na(I) ion is completed by the sulfone O2 located in an adjacent $ZnX_3(6a-\kappa P)$ moiety, related by crystallographic inversion, and also by a methanol molecule and its inversion-related counterpart. The solvating methanol further stabilises the structure through a hydrogen bond with the Zn-bound halide (O1S-H1O...X1, see Figure 7).

The Zn(II) ions in the structures of **8a** and **8b** have the usual, albeit distorted, tetrahedral donor environment (donor set: PX_3), where two Zn-X distances are somewhat shorter than the remaining one ($Zn-X_{1/2} < Zn-X_3$). The associated interligand angles increase in the following order: $X1-Zn-X3 < X2-Zn-P \approx X2-Zn-X3 < X1-Zn-P \approx X1-Zn-X2 < X3-Zn-P$ (cf. the ranges of 102.64(2)-114.50(2)° and 101.61(1)-114.68(3)° for **8a** and **8b**, respectively). In contrast, the sodium cation, as the second metal centre in the structures, has an unsymmetric octahedral coordination (donor set: $cis-X_2O_4$), wherein the extreme Na-donor distances differ by ca. 0.8 and 1.1 Å and the interligand angles (cis -only) span the ranges of 78.25(7)-101.12(8)° and 77.1(1)-104.7(1)° for **8a** and **8b**, respectively. In both cases, the Na atoms appear displaced from the geometrical centre of the octahedron towards O1Sⁱⁱ and O2ⁱ in heavily twisted pseudoequatorial planes {Na, X2, X3, O1Sⁱⁱ, O2ⁱ}. The observed angular distortions of the coordination spheres around both the Zn(II) and Na(I) ions appear to result from an interplay between the unlike metal-donor distances, steric requirements of the individual donors, constraints imposed by the doubly bridged fragments ($Zn(\mu-Br)_2Na$ and $Na(\mu-CH_3OH)_2Na$), and the hydrogen-bond interactions.

As indicated above, the structure of **9a** is very similar to its Na congener **8a**, with the observed differences reflecting the larger size of the alkali metal cation present in the structure. The geometry of the $PZnBr_3$ moiety remains virtually unchanged upon going from **8a** to **9a**; the interligand angles span the range 102.97(1)-113.11(2)° and follow the trend described for **8a** though not with the same differences between the individual values. Although the overall coordination environment of the K^+ ion also remains seemingly the same (cis -interligand angles: 74.02(1)-107.97(5)°), the coordination sphere is expanded because of the longer potassium-donor bonds (by approximately 0.21-0.34 Å in the respective pairs).

The structure of **10a**·CH₃OH (Figure 8, parameters in Table 4) reveals that the replacement of Na⁺ with the Li⁺ ion, which is smaller and prefers tetrahedral coordination environment, results in an opening of the polymeric structure and incorporation of solvent molecules as additional donors into the structure. One of the Li⁺ cations (Li1) is coordinated by a sulfonate oxygen (O2) and three methanol molecules (OnS , $n = 1-3$) constituting a tetrahedral donor set. The other Li⁺ cation (Li2) has a similar coordination, binding two sulfonate oxygens (from different molecules of **6a**), methanol (O4S) and water molecule (O1W).

It is noteworthy that the asymmetric environment of the sulfur atoms renders the structure chiral.

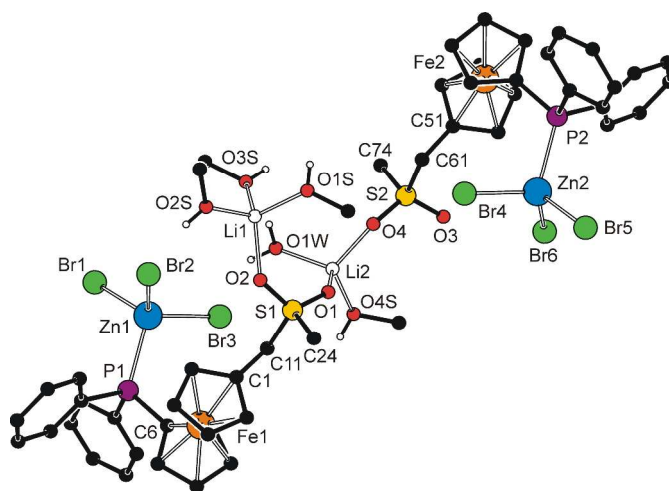


Figure 8. Perspective drawing of the structure of **10a**·CH₃OH. The molecule of solvating methanol and CH hydrogens are omitted for clarity. For a displacement ellipsoid plot, see the ESI (Figure S5).

Table 4. Selected distances and angles for **10a**·CH₃OH (in Å and deg).^a

Zn1-P1	2.437(1)	Zn2-P2	2.442(1)
Zn1-Br1	2.4174(8)	Zn2-Br4	2.3763(8)
Zn1-Br2	2.4016(8)	Zn2-Br5	2.4056(8)
Zn1-Br3	2.4034(8)	Zn2-Br6	2.4362(8)
Li1-O1	1.98(1)	Li2-O1	1.917(8)
Li1-O1S	1.94(1)	Li2-O4	1.907(9)
Li1-O2S	1.911(9)	Li2-O4S	1.916(9)
Li1-O3S	1.962(9)	Li2-O1W	1.92(1)
O-Li1-O	100.9(4)-123.8(5)	O-Li2-O	99.1(4)-114.4(4)
Fe1-C	2.028(6)-2.052(5)	Fe2-C	2.020(6)-2.053(6)
tilt	5.2(3)	tilt	5.5(3)
C1-Cg1-Cg2-C6	-81.6(4)	C1-Cg1-Cg2-C6	82.2(4)
S1-O1	1.433(3)	S2-O3	1.443(4)
S1-O2	1.451(4)	S2-O4	1.454(3)

^a For definitions, see footnote to Table 2.

On the other hand, the halide anion is transferred to the zinc(II) centre, which thus gains a distorted tetrahedral PBr_3 coordination as observed for the Na/K-Zn complexes discussed above. Both $ZnBr_3$ units in the structure of **10a** assume a sterically loose staggered orientation with respect to their bonding PC_3 moieties and do not exert any pronounced angular distortion (cf. the interligand angles ranging 105.64(4)-114.28(4)° for Zn1 and 104.54(3)-112.79(4)° for Zn2).

Conclusion

Alkylation of phosphinoamine **1** with 1,3-propanesultone proceeds selectively under alkylation of the hard nitrogen group to afford the quaternary ammonium salt **2**. Betaine **2**, possessing an intact phosphine substituent, is an attractive functionalised starting material for ferrocenylmethylation reactions with nucleophiles, which was demonstrated in this paper by model reactions leading to **3** and **4**, and by the synthesis of the phosphinosulfones **6** representing new entries

among hybrid³³ phosphinoferrrocene donors possessing flexible methylene spacers.⁶⁻¹¹ Compound **6a**, chosen as a representative phosphinosulfone donor, was shown to form unprecedented³⁴ alkali metal-Zn coordination polymers of the general formula $[\text{ZnMX}_3(\mathbf{6a})(\text{CH}_3\text{OH})]_n$ ($M/X = \text{Na/Br, Na/I, and K/Br}$), in which the ferrocene-based ligand coordinates the softer Zn(II) ion via its phosphine substituent and the alkali metal cation through the sulfone oxygen atoms, while the methanol molecules complete octahedral coordination around the alkali metal ions. These compounds are zwitterions combining negatively charged ZnBr_3 units with cationic centres represented by the alkali metal cations in their structures. In the case of $\text{ZnBr}_2\text{-LiBr}$, the analogous reaction with **6a** provides $[\text{Br}_3\text{Zn}(\mathbf{6a})\text{Li}_2(\text{CH}_3\text{OH})_4(\text{H}_2\text{O})(\mathbf{6a})\text{ZnBr}_3]$ (methanol solvate), a pseudodimeric complex comprising two chemically different, tetrahedral Li^+ centres coordinated by the sulfonate oxygens, solvating methanol and a water molecule, and the phosphine-coordinated ZnBr_3 units.

Experimental

Materials and methods

All reactions were performed under argon atmosphere by standard Schlenk techniques. Amine **1** was prepared as reported previously.¹⁰ Benzene and chloroform were dried by standing over sodium metal and CaH_2 , respectively, and distilled under argon. Dimethyl sulfoxide was distilled under vacuum. Methanol was dried with an in-house PureSolv MD5 solvent-drying system (Innovative Technology, USA). A solution of sodium methoxide was prepared by dissolving the appropriate amount of sodium metal in anhydrous methanol. Other chemicals and solvents were obtained from commercial suppliers (Sigma-Aldrich or Lachner, Czech Republic) and were used without any additional purification.

NMR spectra were recorded at 25 °C on a Varian Unity INOVA spectrometer operating at 399.95 MHz for ^1H , 100.58 MHz for ^{13}C , and 161.92 MHz for ^{31}P . The chemical shifts (δ in ppm) are given relative to internal tetramethylsilane (^1H and ^{13}C) or to external 85% aqueous H_3PO_4 (^{31}P). IR spectra were obtained on a Nicolet Magna 6700 FTIR spectrometer in the range of 400-4000 cm^{-1} . Electrospray ionisation mass spectra (ESI MS) were acquired with a Bruker Esquire 3000 spectrometer using samples dissolved in HPLC-grade methanol.

Syntheses

Synthesis of betaine 2. A solution of propane-1,3-sultone (1.221 g, 10 mmol) in dry benzene (30 mL) was slowly introduced into a solution of amine **1** in the same solvent (4.272 g, 10 mmol in 20 mL). The resultant mixture was stirred at room temperature overnight (15 h), during which time a fine yellow precipitate deposited. The reaction mixture was diluted with methanol (50 mL) and carefully evaporated. The residue was purified by column chromatography over silica gel, eluting first with dichloromethane-methanol (5:1) to remove the less

polar impurities. The polarity of the eluent was then increased (dichloromethane-methanol 3:1) to elute a salt containing the protonated amine **1** as the cation, very likely hydrochloride $[\text{1H}]\text{Cl}$.³⁵ Finally, the eluent was changed to dichloromethane-methanol 1:1, which removed the major orange band of the desired product. Following evaporation and drying under vacuum over sodium hydroxide, betaine **2** was isolated as an air-stable orange solid (4.476 g, 81%). An analytical sample, in the form of the defined solvate $\mathbf{2}\cdot\text{CH}_3\text{OH}$, was obtained upon crystallisation from methanolic solution layered with tetrahydrofuran and diethyl ether.

Analytical data for betaine **2**. ^1H NMR (DMSO-d_6): δ 1.99 (m, 2 H, $\text{NCH}_2\text{CH}_2\text{CH}_2\text{SO}_3$), 2.45 (t, $^3J_{\text{HH}} = 7.1$ Hz, 2 H, $\text{NCH}_2\text{CH}_2\text{CH}_2\text{SO}_3$), 2.78 (s, 6 H, $\text{N}(\text{CH}_3)_2$), 3.21 (m, 2 H, $\text{NCH}_2\text{CH}_2\text{CH}_2\text{SO}_3$), 4.04 (s, 2 H, $\text{C}_5\text{H}_4\text{CH}_2$), 4.16 (vq, $J' = 1.9$ Hz, 2 H, PC_5H_4), 4.22 (vt, $J' = 1.9$ Hz, 2 H, $\text{CH}_2\text{C}_5\text{H}_4$), 4.44 (vt, $J' = 1.9$ Hz, 2 H, $\text{CH}_2\text{C}_5\text{H}_4$), 4.53 (vt, $J' = 1.9$ Hz, 2 H, PC_5H_4), 7.30-7.43 (m, 10 H, PPh_2). $^{31}\text{P}\{^1\text{H}\}$ NMR (DMSO-d_6): δ -18.1 (s). $^{13}\text{C}\{^1\text{H}\}$ NMR (DMSO-d_6): δ 18.89 (s, $\text{NCH}_2\text{CH}_2\text{CH}_2\text{SO}_3$), 47.63 (s, $\text{NCH}_2\text{CH}_2\text{CH}_2\text{SO}_3$), 48.86 (s, NMe_2), 62.03 (s, $\text{NCH}_2\text{CH}_2\text{CH}_2\text{SO}_3$), 63.04 (s, $\text{C}_5\text{H}_4\text{CH}_2$), 71.04 (s, CH of $\text{CH}_2\text{C}_5\text{H}_4$), 71.95 (d, $^3J_{\text{PC}} = 4$ Hz, $\beta\text{-CH}$ of PC_5H_4), 72.86 (s, CH of $\text{CH}_2\text{C}_5\text{H}_4$), 73.35 (s, C_{ipso} of $\text{CH}_2\text{C}_5\text{H}_4$), 73.48 (d, $^2J_{\text{PC}} = 15$ Hz, $\alpha\text{-CH}$ of PC_5H_4), 76.68 (d, $^1J_{\text{PC}} = 9$ Hz, C_{ipso} of PC_5H_4), 128.33 (d, $^3J_{\text{PC}} = 7$ Hz, CH_{meta} of PPh_2), 128.71 (s, CH_{para} of PPh_2), 133.00 (d, $^2J_{\text{PC}} = 20$ Hz, CH_{ortho} of PPh_2), 138.33 (d, $^1J_{\text{PC}} = 10$ Hz, C_{ipso} of PPh_2). IR (Nujol): ν_{max} 3420 br m, 2723 vw, 2669 vw, 1656 m, 1649 m, 1643 m, 1584 w, 1568 vw, 1308 m, 1189 br vs ($\nu_s(\text{SO}_3)$), 1094 m, 1069 m, 1037 vs ($\nu_s(\text{SO}_3)$), 998 m, 920 w, 889 m, 842 m, 820 m, 743 s, 727 m, 697 s, 634 w, 619 w, 602 m, 570 w, 548 w, 523 m, 501 m, 489 m, 456 m, 408 vw cm^{-1} . MS (ESI+): m/z 383 ($[\text{Ph}_2\text{PfcCH}_2]^+$), 550 ($[\text{Ph}_2\text{PfcCH}_2\text{NMe}_2(\text{CH}_2)_3\text{SO}_3 + \text{H}]^+$), 572 ($[\text{Ph}_2\text{PfcCH}_2\text{NMe}_2(\text{CH}_2)_3\text{SO}_3 + \text{Na}]^+$), 588 ($[\text{Ph}_2\text{PfcCH}_2\text{NMe}_2(\text{CH}_2)_3\text{SO}_3 + \text{K}]^+$). Anal. calc. for $\text{C}_{28}\text{H}_{32}\text{FeNO}_3\text{PS}\cdot\text{MeOH}$ (581.5): C 59.90, H 6.24, N 2.41%. Found: C 59.66, H 5.84, N 2.39%.

Preparation of alcohol 3. Degassed aqueous NaOH (25 mL of 2 M solution) was slowly added to a solution of betaine **2** (1.099 g, 2.0 mmol) in dimethyl sulfoxide (25 mL) heated in an oil bath maintained at 130 °C. The refluxing reaction mixture was stirred for 1 h, during which time it darkened and deposited as a brown precipitate. The mixture was cooled to room temperature and diluted with water (50 mL), and the resulting mixture was extracted with dichloromethane (3× 50 mL). The combined organic layers were washed with water (2× 200 mL), dried over magnesium sulfate, and evaporated. The residue was purified by column chromatography on a silica-gel column. Elution with diethyl ether-hexane (1:10) resulted in a yellow band that contained compound **5**, which was isolated in a 6% yield (44 mg) after evaporation. Subsequent elution with diethyl ether-hexane 2:1 led to the development of a major orange band due to alcohol **3**, which was isolated as slowly crystallising orange oil upon evaporation under vacuum. Yield of **3**: 511 mg (64%). The compound was identified by NMR spectroscopy.^{12a}

Analytical data for **5**. ^1H NMR (CDCl_3): δ 1.81 (s, 3 H, CH_3), 3.92 (vt, $J = 1.8$ Hz, 2 H), 3.99 (vt, $J = 1.8$ Hz, 2 H), 4.00 (vt, $J = 1.9$ Hz, 2 H) and 4.29 (vt, $J = 1.9$ Hz, 2 H) ($4 \times \text{CH}$ of C_5H_4), 7.28-7.40 (m, 10 H, $\text{P}(\text{C}_6\text{H}_5)_2$) ppm. $^{31}\text{P}\{^1\text{H}\}$ NMR (CDCl_3): δ -16.0 (s) ppm. $^{13}\text{C}\{^1\text{H}\}$ NMR (CDCl_3): δ 14.40 (s, CH_3), 68.41 (s, CH of MeC_5H_4), 70.23 (s, CH of MeC_5H_4), 71.66 (d, $^3J_{\text{PC}} = 4$ Hz, CH of PC_5H_4), 73.45 (d, $^2J_{\text{PC}} = 15$ Hz, CH of MeC_5H_4), 84.67 (s, C_{ipso} of MeC_5H_4), 128.07 (d, $^3J_{\text{PC}} = 7$ Hz, CH_{meta} in PPh_2), 128.40 (s, CH_{para} in PPh_2), 133.51 (d, $^2J_{\text{PC}} = 20$ Hz, CH_{ortho} in PPh_2), 139.22 (d, $^1J_{\text{PC}} = 10$ Hz, C_{ipso} in PPh_2) ppm. The signal of C_{ipso} of PC_5H_4 is probably obscured by the solvent resonance. MS (ESI+): m/z 200 ($[\text{FcCH}_3]^+$), 384 ($[\text{Ph}_2\text{PfcCH}_3]^+$). Anal. calc. for $\text{C}_{23}\text{H}_{21}\text{FeP}$ (400.2): C 71.89, H 5.51%. Found: C 71.72, H 5.41%.

Preparation of ether 4. Betaine **2** (1.101 g, 2.0 mmol) was dissolved in dimethyl sulfoxide (25 mL) at 100 °C, and the solution was treated with 2 M MeONa in methanol (25 mL). The resulting mixture was heated under reflux for 2 h and cooled to room temperature. Then, it was diluted with water (50 mL) and extracted with dichloromethane (3×50 mL). The organic extracts were washed with water (2×200 mL), dried over magnesium sulfate, and evaporated. The crude product was purified by chromatography over a silica-gel column using diethyl ether-hexane 1:1 as the eluent. The major band due to the product was collected and evaporated under vacuum to yield ether **4** as a yellow-orange solid. Yield: 388 mg (47%). The NMR spectra of the product were identical with those reported in the literature.⁹

Preparation of 6a. A solution of sodium methanesulfinate (0.534 g, 5.0 mmol) in degassed water (25 mL) was added to a solution of betaine **2** (1.097 g, 2.0 mmol) in dimethylsulfoxide (25 mL) kept in an oil bath preheated to 130 °C. The resulting solution was heated under reflux for 2 h, whereupon it turned brown, and a yellow-brown precipitate separated. The reaction mixture was cooled to room temperature, diluted with water (50 mL), and extracted with dichloromethane (3×50 mL). The combined organic layers were diluted with dichloromethane (50 mL), washed with water (2×200 mL), dried over anhydrous magnesium sulfate, and evaporated under reduced pressure. The residue was purified by chromatography over a silica-gel column, first using dichloromethane-methanol 50:1 to elute the main orange band of **6a** and a small tailing band containing alcohol **3**. The mobile phase was then changed to dichloromethane-methanol 20:1, which led to the development of an additional broad yellow band containing the side product **7**. The complete separation of **3** and **6a** was achieved through additional chromatography over silica gel using ethyl acetate-hexane (1:2) as the eluent (note: the alcohol elutes first under such conditions) or, alternatively, via crystallisation from ethyl acetate/hexane. Yields: **6a** – yellow solid (272 mg, 29%); **3** – orange, slowly crystallising oil (14 mg, 2%); and **7** – rusty brown oil (74 mg, 12%).

Analytical data for **6a**. ^1H NMR (CDCl_3): δ 2.62 (s, 3 H, SO_2Me), 3.59 (s, 2 H, $\text{C}_5\text{H}_4\text{CH}_2$), 4.10 (vt, $J = 1.8$ Hz, 2 H), 4.19 (vt, $J = 1.9$ Hz, 2 H), 4.26 (vt, $J = 1.9$ Hz, 2 H) and 4.40 (vt, $J = 1.8$ Hz, 2 H) ($4 \times \text{CH}$ in fc); 7.31-7.41 (m, 10 H, PPh_2).

$^{31}\text{P}\{^1\text{H}\}$ NMR (CDCl_3): δ -17.0 (s). $^{13}\text{C}\{^1\text{H}\}$ NMR (CDCl_3): δ 38.43 (SO_2Me), 56.65 (s, $\text{C}_5\text{H}_4\text{CH}_2$), 70.59 (s, CH of $\text{CH}_2\text{C}_5\text{H}_4$), 71.07 (s, CH of $\text{CH}_2\text{C}_5\text{H}_4$), 71.73 (d, $^3J_{\text{PC}} = 4$ Hz, β - CH of PC_5H_4), 74.03 (d, $^2J_{\text{PC}} = 15$ Hz, α - CH of PC_5H_4), 74.88 (s, C_{ipso} of $\text{CH}_2\text{C}_5\text{H}_4$), 128.31 (d, $^3J_{\text{PC}} = 7$ Hz, CH_{meta} of PPh_2), 128.80 (s, CH_{para} of PPh_2), 133.50 (d, $^2J_{\text{PC}} = 20$ Hz, CH_{ortho} of PPh_2), 138.67 (d, $^1J_{\text{PC}} = 10$ Hz, C_{ipso} of PPh_2). The resonance of ferrocene C-P was not found. IR (Nujol): ν_{max} 3015 m, 2725 vw, 2282 vw, 1583 w, 1567 vw, 1435 s, 1419 w, 1412 w, 1397 w, 1322 m, 1304 vs ($\nu_{\text{as}}(\text{SO}_2)$), 1286 m, 1242 w, 1228 w, 1192 w, 1161 m, 1139 vs ($\nu_{\text{s}}(\text{SO}_2)$), 1122 m, 1099 m, 1084 vw, 1069 w, 1058 vw, 1038 m, 1023 m, 998 w, 963 s, 928 m, 903 vw, 843 m, 835 m, 788 s, 750 s, 742 vs, 704 s, 697 vs, 630 w, 618 vw, 603 w, 569 vw, 529 m, 510 m, 486 s, 479 vs, 455 s, 441 m, 406 vw cm^{-1} . MS (ESI+): m/z 383 ($[\text{Ph}_2\text{PfcCH}_2]^+$), 463 ($[\text{6a} + \text{H}]^+$), 485 ($[\text{6a} + \text{Na}]^+$), 501 ($[\text{6a} + \text{K}]^+$). Anal. calc. for $\text{C}_{24}\text{H}_{23}\text{FeO}_2\text{PS}$ (462.3): C 62.35, H 5.01%. Found: C 62.59, H 4.82%.

Analytical data for **7**. ^1H NMR (CDCl_3): δ 3.59 (d, $^2J_{\text{PH}} = 12.7$ Hz, 2 H, PCH_2), 3.83 (d of vt, $J = 1.9$, 0.8 Hz, 2 H), 3.94 (vt, $J = 1.9$ Hz, 2 H), 4.02 (vt, $J = 1.9$ Hz, 2 H) and 4.33 (vt, $J = 1.9$ Hz, 2 H) ($4 \times \text{CH}$ in fc); 6.12 (m, 2 H, α - CH of $\text{P}=\text{C}_5\text{H}_4$), 6.40 (m, 2 H, β - CH of $\text{P}=\text{C}_5\text{H}_4$), 7.25-7.35 (m, 10 H, fcPPh_2), 7.41-7.47 (m, 8 H, CH_{ortho} and CH_{meta} of CH_2PPh_2), 7.55-7.61 (m, 2 H, CH_{para} of CH_2PPh_2). $^{31}\text{P}\{^1\text{H}\}$ NMR (CDCl_3): δ -16.9 (s, fcPPh_2), 10.1 (s, $\text{CH}_2\text{P}=\text{C}_5\text{H}_4$). $^{13}\text{C}\{^1\text{H}\}$ NMR (CDCl_3): δ 30.01 (dd, $^1J_{\text{PC}} = 53$ Hz, $J_{\text{PC}} = 1$ Hz, PCH_2), 69.50 (s, CH of fc), 71.49 (s, CH of fc), 71.77 (d, $^3J_{\text{PC}} = 4$ Hz, CH of fc), 73.89 (d, $^2J_{\text{PC}} = 15$ Hz, CH of fc), 77.42 (d, $^2J_{\text{PC}} = 2$ Hz, C_{ipso} of fc), 78.21 (d, $^1J_{\text{PC}} = 110$ Hz, C_{ipso} of $\text{P}=\text{C}_5\text{H}_4$), 113.92 (d, $^2J_{\text{PC}} = 18$ Hz, α - CH of $\text{P}=\text{C}_5\text{H}_4$), 115.83 (d, $^3J_{\text{PC}} = 15$ Hz, β - CH of $\text{P}=\text{C}_5\text{H}_4$), 125.49 (d, $^1J_{\text{PC}} = 86$ Hz, C_{ipso} of CH_2PPh_2), 128.19 (d, $^3J_{\text{PC}} = 7$ Hz, CH_{meta} of CH_2PPh_2), 128.59 (d, $^2J_{\text{PC}} = 12$ Hz, CH_{ortho} of fcPPh_2), 128.63 (s, CH_{para} of fcPPh_2), 132.54 (d, $^4J_{\text{PC}} = 3$ Hz, CH_{para} of CH_2PPh_2), 133.37 (s, CH_{meta} of fcPPh_2), 133.52 (d, $^2J_{\text{PC}} = 10$ Hz, CH_{ortho} of CH_2PPh_2), 138.85 (d, $^1J_{\text{PC}} = 10$ Hz, C_{ipso} of fcPPh_2). MS (ESI+): m/z 383 ($[\text{Ph}_2\text{PfcCH}_2]^+$), 633 ($[\text{7} + \text{H}]^+$). HR MS (APCI+) calc. for $\text{C}_{40}\text{H}_{35}\text{FeP}_2$ ($[\text{M} + \text{H}]^+$): 633.1558, found: 633.1561. Anal. calc. for $\text{C}_{40}\text{H}_{34}\text{FeP}_2 \cdot 1/8\text{CHCl}_3$ (647.4): C 74.44, H 5.31%. Found: C 74.30, H 5.38%.

Preparation of 6b. Betaine **2** (2.0 mmol) was dissolved in dimethylsulfoxide (25 mL), and the reaction flask was transferred to an oil-bath preheated to 130 °C. After stirring for several minutes at this temperature, an aqueous solution of the corresponding sulfinate (5.0 mmol in 25 mL of degassed water) was added, and the resultant mixture was heated under reflux for 2 h (an orange precipitate separated). The reaction mixture was cooled to room temperature, diluted with water (50 mL), and extracted with dichloromethane (3×50 mL). The combined organic layers were diluted with dichloromethane (50 mL), washed with water (2×200 mL), dried over magnesium sulfate, and evaporated under vacuum. The products were isolated by column chromatography over silica gel. Initial elution with dichloromethane-methanol 50:1 produced a major orange band due to sulfone **6**, followed by a minor band of

alcohol **3**. Subsequent elution with dichloromethane-methanol 20:1 led to the development of a broad yellow band containing crude **7**. Compound **3** was further purified as described above (see the preparation of **3**). Particular details are as follows.

The reaction of **2** (1.099 g, 2.0 mmol) with sodium phenylsulfinate (0.838 g, 5.0 mmol) as described above yielded **6b** (yellow solid; 524 mg, 50%), **3** (14 mg, 2%), and **7** (61 mg, 10%). Starting with **2** (1.095 g, 2.0 mmol) and sodium 4-toluenesulfinate (0.937 g, 5.0 mmol), an analogous procedure produced **6c** (yellow solid; 570 mg, 53%), **3** (25 mg, 3%), and **7** (98 mg, 16%).

Analytical data for **6b**. $^1\text{H NMR}$ (CDCl_3): δ 3.68 (s, 2 H, $\text{C}_5\text{H}_4\text{CH}_2$), 3.94 (vt, $J = 1.9$ Hz, 2 H), 4.02 (vq, $J = 1.8$ Hz, 2 H), 4.05 (vt, $J = 1.9$ Hz, 2 H) and 4.32 (vt, $J = 1.8$ Hz, 2 H) ($4\times$ CH of fc), 7.28-7.35 (m, 10 H, PPh_2), 7.42-7.47 (m, 2 H, SO_2Ph), 7.57-7.62 (m, 3 H, SO_2Ph). $^{31}\text{P}\{^1\text{H}\}$ NMR (CDCl_3): δ -16.9 (s). $^{13}\text{C}\{^1\text{H}\}$ NMR (CDCl_3): δ 58.23 (s, $\text{C}_5\text{H}_4\text{CH}_2$), 70.16 (s, CH of $\text{CH}_2\text{C}_5\text{H}_4$), 71.30 (s, CH of $\text{CH}_2\text{C}_5\text{H}_4$), 71.52 (d, $^3J_{\text{PC}} = 4$ Hz, β -CH of PC_5H_4), 73.81 (d, $^2J_{\text{PC}} = 15$ Hz, α -CH of PC_5H_4), 74.68 (s, C_{ipso} of $\text{CH}_2\text{C}_5\text{H}_4$), 76.79 (d, $^1J_{\text{PC}} = 7$ Hz, C_{ipso} of PC_5H_4), 128.24 (d, $^3J_{\text{PC}} = 7$ Hz, CH_{meta} of PPh_2), 128.69 (s, CH_{ortho} and CH_{meta} of $\text{SO}_2\text{Ph} + \text{CH}_{\text{para}}$ of PPh_2), 133.44 (d, $^2J_{\text{PC}} = 20$ Hz, CH_{ortho} of PPh_2), 133.51 (s, CH_{para} of SO_2Ph), 137.84 (s, C_{ipso} of SO_2Ph), 138.73 (d, $^1J_{\text{PC}} = 10$ Hz, C_{ipso} of PPh_2). IR (Nujol): ν_{max} 2723 vw, 2667 vw, 1583 vw, 1568 vw, 1400 w, 1311 s, 1304 vs ($\nu_{\text{as}}(\text{SO}_2)$), 1288 m, 1263 w, 1240 vw, 1223 vw, 1149 vs, ($\nu_{\text{s}}(\text{SO}_2)$), 1110 w, 1086 m, 1068 w, 1058 vw, 1036 w, 1029 m, 999 vw, 974 vw, 927 w, 888 vw, 880 vw, 871 vw, 834 m, 761 m, 749 s, 708 m, 700 m, 686 m, 633 w, 614 w, 571 s, 549 vw, 531 w, 503 s, 490 s, 458 m, 432 vw, cm^{-1} . MS (ESI+): m/z 383 ($[\text{Ph}_2\text{PfcCH}_2]^+$), 525 ($[\text{6b} + \text{H}]^+$), 547 ($[\text{6b} + \text{Na}]^+$), 563 ($[\text{6b} + \text{K}]^+$). Anal. calc. for $\text{C}_{29}\text{H}_{25}\text{FeO}_2\text{PS}$ (524.4): C 66.42, H 4.81%. Found: C 66.20, H 4.80%.

Analytical data for **6c**. $^1\text{H NMR}$ (CDCl_3): δ 2.43 (s, 3 H, $\text{C}_6\text{H}_4\text{CH}_3$), 3.67 (s, 2 H, $\text{C}_5\text{H}_4\text{CH}_2$), 3.95 (vt, $J = 1.9$ Hz, 2 H), 4.02 (vq, $J = 1.8$ Hz, 2 H), 4.06 (vt, $J = 1.9$ Hz, 2 H) and 4.32 (vt, $J = 1.8$ Hz, 2 H) ($4\times$ CH of fc), 7.23-7.26 (m, 2 H, C_6H_4), 7.29-7.35 (m, 10 H, PPh_2), 7.46-7.50 (m, 2 H, C_6H_4). $^{31}\text{P}\{^1\text{H}\}$ NMR (CDCl_3): δ -16.9 (s). $^{13}\text{C}\{^1\text{H}\}$ NMR (CDCl_3): δ 21.64 (s, $\text{C}_6\text{H}_4\text{CH}_3$), 58.28 (s, $\text{C}_5\text{H}_4\text{CH}_2$), 70.14 (s, CH of $\text{CH}_2\text{C}_5\text{H}_4$), 71.33 (s, CH of $\text{CH}_2\text{C}_5\text{H}_4$), 71.50 (d, $^3J_{\text{PC}} = 4$ Hz, β -CH of PC_5H_4), 73.78 (d, $^2J_{\text{PC}} = 14$ Hz, α -CH of PC_5H_4), 74.86 (s, C_{ipso} of $\text{CH}_2\text{C}_5\text{H}_4$), 76.77 (d, $^1J_{\text{PC}} = 7$ Hz, C_{ipso} of PC_5H_4), 128.24 (d, $^3J_{\text{PC}} = 7$ Hz, CH_{meta} of PPh_2), 128.69 (s), 128.71 (s) and 129.32 (s) ($2\times$ CH of $\text{C}_6\text{H}_4 + \text{CH}_{\text{para}}$ of PPh_2), 133.45 (d, $^2J_{\text{PC}} = 20$ Hz, CH_{ortho} of PPh_2), 134.96 (s, CSO_2 of C_6H_4), 138.75 (d, $^1J_{\text{PC}} = 10$ Hz, C_{ipso} of PPh_2), 144.43 (s, CCH_3 of C_6H_4) ppm. IR (Nujol): ν_{max} 2726 vw, 2669 vw, 1594 w, 1436 m, 1403 w, 1319 vs ($\nu_{\text{as}}(\text{SO}_2)$), 1301 m, 1289 m, 1259 m, 1221 m, 1194 vw, 1183 vw, 1148 vs ($\nu_{\text{s}}(\text{SO}_2)$), 1117 w, 1106 m, 1086 s, 1070 w, 1053 vw, 1047 vw, 1038 w, 1027 m, 998 vw, 926 w, 888 w, 875 m, 868 w, 848 vw, 837 m, 824 m, 813 m, 799 w, 750 s, 698 s, 633 m, 611 w, 552 m, 513 s, 497 s, 485 m, 469 w, 453 m, 440 vw, 431 vw cm^{-1} . MS (ESI+): m/z 383 ($[\text{Ph}_2\text{PfcCH}_2]^+$), 539 ($[\text{6c} + \text{H}]^+$), 561 ($[\text{6c} + \text{Na}]^+$). Anal. calc. for $\text{C}_{30}\text{H}_{27}\text{FeO}_2\text{PS}$ (538.4): C 66.92, H 5.06%. Found: 66.62, H 5.00%.

Preparation of 8a. A methanolic solution of sodium bromide (10.3 mg, 0.10 mmol in 0.6 mL) was added to solid ZnBr_2 (22.5 mg, 0.10 mmol), followed by a solution of sulfone **6a** in chloroform (46.2 mg, 0.10 mmol in 0.6 mL). The resulting mixture was stirred for 30 min, filtered through a PTFE syringe filter (0.45 μm pore size), and diluted with additional methanol (0.3 mL) as the top layer. The filtrate was layered with methyl *tert*-butyl ether to a total volume of 10 mL, and the mixture was set aside for crystallisation. The orange crystals, which precipitated over several days, were filtered off, washed three times with methyl *tert*-butyl ether, and dried under vacuum. Yield of **8a**: 64.6 mg (79%).

IR (Nujol): ν_{max} 3495 br m, 3090 m, 2724 vw, 2670 vw, 1618 w, 1433 m, 1410 w, 1354 w, 1317 m, 1303 vs, 1269 m, 1248 vw, 1228 w, 1193 vw, 1169 m, 1145 s, 1119 s, 1096 w, 1065 vw, 1052 vw, 1043 vw, 1030 m, 1022 m, 1006 m, 971 m, 953 w, 931 w, 904 vw, 890 m, 857 w, 847 w, 828 w, 792 w, 751 s, 705 w, 694 m, 629 w, 610 w, 571 vw, 543 w, 518 m, 490 s, 457 m, 434 vw cm^{-1} . MS (ESI+): m/z 383 ($[\text{Ph}_2\text{PfcCH}_2]^+$), 463 ($[\text{6a} + \text{H}]^+$), 485 ($[\text{6a} + \text{Na}]^+$), 501 ($[\text{6a} + \text{K}]^+$). Anal. calc. for $\text{C}_{25}\text{H}_{27}\text{Br}_3\text{FeNaO}_3\text{PSZn}$ (822.4): C 36.51, H 3.31%. Found: C 36.64, H 3.37%.

Preparation of 8b. Compound **8b** was prepared similarly to **8a** but using different amounts of solvents. Thus, a solution of NaI (15.0 mg, 0.10 mmol) in methanol (0.3 mL) and a chloroform solution of **6a** (46.2 mg, 0.10 mmol in 0.6 mL) were successively added to ZnI_2 (31.9 mg, 0.10 mmol). The resultant mixture was stirred for 30 min, filtered (PTFE syringe filter as above), and layered with methanol (0.1 mL) and methyl *tert*-butyl ether (up to 10 mL total volume). Crystallisation by diffusion over several days produced an orange crystalline solid, which was filtered off, washed three times with methyl *tert*-butyl ether, and dried under vacuum. Yield: 78.4 mg (81%).

IR (Nujol): ν_{max} 3490 br m, 3099 w, 3091 m, 2724 vw, 2670 vw, 1618 w, 1435 m, 1407 w, 1314 m, 1299 vs, 1267 m, 1227 w, 1192 w, 1166 m, 1143 s, 1118 m, 1107 m, 1095 m, 1090 m, 1062 w, 1052 vw, 1042 w, 1030 m, 1021 m, 1000 m, 970 m, 953 w, 931 w, 887 m, 879 w, 854 w, 847 w, 834 w, 828 w, 790 w, 774 vw, 749 s, 704 w, 692 m, 627 w, 608 w, 570 w, 541 w, 517 m, 499 m, 490 s, 457 m, 432 vw cm^{-1} . MS (ESI+): m/z 383 ($[\text{Ph}_2\text{PfcCH}_2]^+$), 463 ($[\text{6a} + \text{H}]^+$), 485 ($[\text{6a} + \text{Na}]^+$), 501 ($[\text{6a} + \text{K}]^+$). Anal. Calc. for $\text{C}_{25}\text{H}_{27}\text{FeI}_3\text{NaO}_3\text{PSZn}$ (963.4): C 31.17, H 2.82%. Found: C 31.44, H 2.86%.

Synthesis of 9a. Using an analogous procedure, a solution of KBr (11.9 mg, 0.10 mmol) in methanol (1.6 mL) was added to solid ZnBr_2 (22.6 mg, 0.10 mmol) followed by a chloroform solution of **6a** (46.3 mg, 0.10 mmol in 0.4 mL). The resulting mixture was stirred for 30 min and filtered through a PTFE syringe filter. The filtrate was diluted with methanol (0.5 mL) and layered with methyl *tert*-butyl ether (up to total volume of 10 mL). Crystallisation by liquid-phase diffusion afforded **9a** as orange crystals, which were isolated as above. Yield: 36.7 mg (44%). Note: some unreacted KBr typically remains on the walls of the reaction vessel as a fine white precipitate.

IR (Nujol): ν_{\max} 3475 br m, 3089 m, 1619 w, 1433 m, 1407 w, 1318 m, 1293 s, 1267 m, 1228 w, 1193 w, 1167 m, 1146 s, 1118 m, 1107 m, 1091 m, 1064 w, 1052 vw, 1043 w, 1030 m, 1021 m, 1013 s, 971 m, 960 m, 931 w, 905 w, 890 m, 881 w, 857 w, 846 w, 826 w, 790 w, 748 s, 704 w, 692 s, 627 w, 610 w, 543 w, 517 m, 499 s, 489 s, 459 s, 409 w cm^{-1} . Anal. Calc. for $\text{C}_{25}\text{H}_{27}\text{Br}_3\text{FeKO}_3\text{PSZn}$ (838.5): C 35.81, H 3.25 %. Found: C 35.61, H 3.29 %.

Preparation of 10a. ZnBr_2 (22.6 mg, 0.10 mmol) and LiBr (8.7 mg, 0.10 mmol) were dissolved in methanol (0.10 mL). A chloroform solution of ligand **6a** (46.3 mg, 0.10 mmol in 0.4 mL) was added and the resultant mixture was stirred for 30 min. Filtration, addition of methanol (0.1 mL), addition of methyl *tert*-butyl ether (up to 10 mL total volume) and crystallisation as described above gave **10a** as an orange crystalline solid, which was isolated by suction, washed with methyl *tert*-butyl ether, and dried under vacuum. Yield: 42.8 mg (49 %).

IR (Nujol): ν_{\max} ca. 3270-3650 m composite, 3086 w, 1708 w, 1623 br s, 1403 w, 1318 m, 1306 w, 1283 s, 1263 m, 1247 w, 1228 w, 1193 vw, 1168 m, 1143 s, 1116 s, 1095 m, 1062 w, 1041 w, 1030 m, 1020 m, 973 m, 930 w, 888 s, 857 w, 876 w, 833 vw, 828 vw, 790 m, 748 vs, 705 w, 692 w, 627 w, 609 w, 542 w, 517 m, 489 br s, 459 s cm^{-1} . Anal. Calc. for $\text{Li}_2\text{Zn}_2\text{Br}_6(\mathbf{6a})_2(\text{MeOH})_5(\text{H}_2\text{O})_3$ (1762.9): C 36.11, H 4.12 %. Found: C 35.88, H 3.79 % (the sample is slightly hygroscopic).

X-ray crystallography

The diffraction data ($\theta_{\max} = 27.5^\circ$; data completeness $\geq 99.3\%$) were recorded with a Nonius Kappa diffractometer equipped with an APEX-II CCD detector (Bruker) and a Cryostream Cooler (Oxford Cryosystems) at 150(2) K using graphite monochromatized $\text{Mo K}\alpha$ radiation ($\lambda = 0.71073 \text{ \AA}$) and were corrected for absorption using routines included in the diffractometer software.

The structures were solved by the direct methods (SHELXS97) and refined by full-matrix least squares routines based on F^2 (SHELXL97).³⁶ The non-hydrogen atoms were refined with anisotropic displacement parameters. The hydrogen atoms residing on the oxygen atoms (OH protons) in the structures of **2-CH₃OH**, **8a**, **8b**, and **9a** were identified on the difference electron density maps and refined as riding atoms with $U_{\text{iso}}(\text{H})$ set to 1.2-times $U_{\text{eq}}(\text{O})$. In the case of **10a**· CH_3OH , they were placed into positions suitable for the formation of hydrogen bonds and refined similarly. Hydrogen atoms residing on the carbon atoms were included in their theoretical positions and refined analogously.

Description of the crystallization experiments and a listing of relevant crystallographic data and structure refinement parameters are available in the ESI (Table S1). Geometric data as well as all structural drawings were obtained with a recent version of the PLATON program.³⁷ All numerical values are rounded with respect to their estimated standard deviations (ESDs) given with one decimal. Parameters pertaining to atoms in constrained positions are presented without ESDs.

Acknowledgements

Results reported in this paper were obtained with financial support from the Czech Science Foundation (project no. 15-11571S) and the Grant Agency of Charles University in Prague (project no. 8415).

Notes and references

^a Department of Inorganic Chemistry, Faculty of Science, Charles University in Prague, Hlavova 2030, 128 40 Prague, Czech Republic. E-mail address: stepnic@natur.cuni.cz.

† Electronic Supplementary Information (ESI) available: A comparison of the IR spectra of **6a**, **8a**, and **8b** in the fingerprint region, additional structural drawings for **8a** and **8b**, and a summary of the crystallographic data and structure refinement parameters (Table S1). CCDC 1401233-1401241, 1410159, and 1410160. See DOI: 10.1039/x0xx00000x/

- a) T. J. Kealy and P. L. Pauson, *Nature*, 1951, **168**, 1039; b) S. A. Miller, J. A. Tebboth and J. F. Tremaine, *J. Chem. Soc.*, 1952, 632.
- a) G. Wilkinson, M. Rosenblum, M. C. Whiting and R. B. Woodward, *J. Am. Chem. Soc.*, 1952, **74**, 2125; b) E. O. Fischer and W. Pfab, *Z. Naturforsch.*, 1952, **7b**, 377.
- a) E. G. Perevalova, M. D. Reschetova and K.I. Grandberg (Eds.), *Methods of Organoelement Compounds*, volume *Organoiron Compounds*, Ferrocene, Nauka, Moscow, 1983 (in Russian); b) V. I. Boev, L. V. Snegur, V. N. Babin and Yu. S. Nekrasov, *Usp. Khim.*, 1997, **66**, 677; c) A. Togni and T. Hayashi (Eds.), *Ferrocenes*, VCH, Weinheim, 1995, p. 677 ff.; d) B. W. Rockett and G. Marr, *J. Organomet. Chem.*, 1991, **416**, 327 and previous "Annual surveys of ferrocene chemistry."
- R. Gleiter, C. Bleiholder and F. Rominger, *Organometallics*, 2007, **26**, 4850.
- a) *Ferrocenes: Ligands, Materials and Biomolecules*, P. Štěpnička (Ed.), Wiley, Chichester, 2008; b) R. C. J. Atkinson, V. C. Gibson and N. J. Long, *Chem. Soc. Rev.*, 2004, **33**, 313; c) R. Gómez Arrayás, J. Adrio and J. C. Carretero, *Angew. Chem., Int. Ed.*, 2006, **45**, 7674.
- A proper choice of the alkylation reagent can sometimes eliminate this problem. For an example, see: P. Štěpnička and I. Čiřařová, *Organometallics*, 2003, **22**, 1728.
- M. Widhalm, U. Nettekoven and K. Mereiter, *Tetrahedron: Asymmetry*, 1999, **10**, 4369.
- a) A. Labande, J.-C. Daran, E. Manoury and R. Poli, *Eur. J. Inorg. Chem.*, 2007, 1205; b) S. Gülcemal, A. Labande, J.-C. Daran, B. Çetinkaya and R. Poli, *Eur. J. Inorg. Chem.*, 2009, 1806; c) A. Labande, N. Debono, A. Sourmia-Saquet, J.-C. Daran and R. Poli, *Dalton Trans.*, 2013, **42**, 6531.
- P. Štěpnička and I. Čiřařová, *Dalton Trans.*, 2013, **42**, 3373.
- P. Štěpnička, M. Zábranský and I. Čiřařová, *ChemistryOpen*, 2012, **1**, 71.
- For an alternative synthesis of **1**, see M. E. Wright, *Organometallics*, 1990, **9**, 853.
- a) P. Štěpnička and T. Baše, *Inorg. Chem. Commun.*, 2001, **4**, 682; b) P. Štěpnička, I. Čiřařová and J. Schulz, *Organometallics*, 2011, **30**, 4393; c) P. Štěpnička, J. Schulz, T. Klemann, U. Siemeling and I.

- Cišařová, *Organometallics*, 2010, **29**, 3187; d) U. Siemeling, T. Klemann, C. Bruhn, J. Schulz and P. Štěpnička, *Dalton Trans.*, 2011, **40**, 4722; e) P. Štěpnička and I. Cišařová, *J. Organomet. Chem.*, 2012, **716**, 110.
- 13 V. I. Boev, *Zh. Obshch. Khim.*, 1991, **61**, 1174.
- 14 In addition to the betaine, the reaction of **1** with the sultone gives rise to other products, namely salt(s) with protonated amines (presumably hydrochloride), which are less polar than **2**, and some P-alkylated products (δ_p 26.7; more polar than **2**).
- 15 a) W. Henderson, A. G. Oliver and A. J. Downard, *Polyhedron*, 1996, **15**, 1165; b) Yu. S. Nekrasov, R. S. Skazov, A. A. Simenel, L. V. Snegur and I. V. Kachala, *Russ. Chem. Bull.*, 2006, **55**, 1368.
- 16 J. K. Lindsay and C. R. Hauser, *J. Org. Chem.*, 1957, **22**, 355.
- 17 a) M. Uher and Š. Toma, *Collect. Czech. Chem. Commun.*, 1971, **36**, 3056; b) J. B. Evans and G. Marr, *J. Chem. Soc., Perkin Trans. I*, 1972, 2502; c) V. I. Boev and A. V. Dombrovskii, *Zh. Obshch. Khim.*, 1984, **54**, 1863.
- 18 J. H. Brownie, M. C. Baird and H. Schmider, *Organometallics*, 2007, **26**, 1433.
- 19 K.-S. Gan and T. S. A. Hor in *Ferrocenes: Heterogeneous Catalysis, Organic Synthesis, Materials Science*, chapter 1.3, pp. 19, VCH, Weinheim, 1995.
- 20 P. A. Chaloner, R. M. Harrison, P. B. Hitchcock and R. T. Pedersen, *Acta Crystallogr., Sect. C: Cryst. Struct. Commun.*, 1992, **48**, 717.
- 21 P. C. Healy, W. A. Loughlin, B. M. Sweeney and I. D. Jenkins, *Acta Crystallogr., Sect. E, Struct. Rep. Online*, 2002, **58**, o137. The distances and angles were calculated from coordinates deposited in the Cambridge Crystallographic Database (refcode: MIFSID).
- 22 F. A. M. Rudolph, A. L. Fuller, A. M. Z. Slawin, M. Bühl, R. A. Aitken and J. D. Woollins, *J. Chem. Crystallogr.*, 2010, **40**, 253.
- 23 C. Lichtenberg, N. S. Hillesheim, M. Elfferding, B. Oelkers and J. Sundermeyer, *Organometallics*, 2012, **31**, 4259.
- 24 I. R. Butler, W. R. Cullen, F. W. B. Einstein and A. C. Willis, *Organometallics*, 1985, **4**, 603.
- 25 J. C. J. Bart, *J. Chem. Soc. B*, 1969, 350.
- 26 W. E. McEwen, C. E. Sullivan and R. O. Day, *Organometallics*, 1983, **2**, 420.
- 27 R. G. Pearson, *J. Am. Chem. Soc.*, 1963, **85**, 3533.
- 28 R. H. Prince, Zinc and Cadmium in *Comprehensive Coordination Chemistry*, ed. G. Wilkinson, R. D. Gillard and J. A. McCleverty, vol. 5, ch. 56.1, pp. 925-1097, Pergamon, Oxford, 1987.
- 29 The Na⁺ necessary for the formation of **8a** seems to have come from the commercial ZnBr₂ sample, which was shown to contain 0.04 μg Na per 1 mg by atomic absorption spectrometry, or simply from the solvents and/or the glassware.
- 30 Increasing the chloroform-to-methanol ratio can result in a separation of the alkali metal halide (MX) from the reaction mixture (full or partial), which in turn reduces the yield of the mixed-metal complex or even fully prevents its formation. On the other hand, a low chloroform-to-methanol ratio (i.e., more polar reaction mixture) can significantly reduce the yield of the desired mixed-metal complex by increasing its solubility.
- 31 We feel that compound **10a** need not necessarily be the only product possibly arising in the **6a**/LiBr/ZnBr₂ system as the reaction can, in principle, afford also other, differently solvated species.
- 32 See, for instance: a) A. Santoro and A. D. Mighell, *Acta Crystallogr., Sect. A: Found. Crystallogr.*, 1970, **26**, 124; b) V. Balashov and H. D. Ursell, *Acta Crystallogr.*, 1957, **10**, 582; c) J. D. H. Donnay, *Am. Mineral.*, 1943, **28**, 507.
- 33 (a) A. Bader and E. Lindner, *Coord. Chem. Rev.*, 1991, **108**, 27; (b) C. S. Slone, D. A. Weinberger and C. A. Mirkin, *Progr. Inorg. Chem.*, 1999, **48**, 233.
- 34 The search for structurally characterised compounds combining octahedral Na(I) and tetrahedral Zn(II) sites in the Cambridge Structural Database, version 5.36 of November 2014 with updates from November 2014, resulted in 42 hits. These compounds were mostly coordination polymers featuring various O-donors. None of them contained phosphine donors or motifs similar to that encountered in **8a** and **8b**.
- 35 Dissolution of this by-product in dichloromethane, washing with 5% aqueous NaOH, and subsequent chromatographic purification recovered pure **1**.
- 36 G. M. Sheldrick, *Acta Crystallogr., Sect. A: Found. Crystallogr.*, 2008, **64**, 112.
- 37 A. L. Spek, *J. Appl. Crystallogr.*, 2003, **36**, 7.

ARTICLE

Table 2. Selected geometric parameters of the molecules of phosphinosulfones **6** (in Å and deg.).

Parameter ^a	6a	6a'	6b	6c
Fe-C	2.031(2)-2.060(2)	2.035(2)-2.054(2)	2.026(1)-2.058(2)	2.040(2)-2.056(2)
tilt	2.98(9)	3.3(1)	2.64(9)	1.9(1)
C1-Cg2-Cg2-C6	-79.1(1)	162.5(1)	128.2(1)	73.3(1)
P-C6	1.817(2)	1.821(2)	1.812(2)	1.815(2)
P-C12	1.838(2)	1.835(2)	1.832(2)	1.835(2)
P-C18	1.839(2)	1.832(2)	1.834(2)	1.834(2)
C1-C11	1.494(2)	1.494(3)	1.488(2)	1.489(3)
C11-S	1.786(2)	1.781(2)	1.784(2)	1.792(2)
S-O1	1.435(1)	1.432(2)	1.446(1)	1.440(2)
S-O2	1.439(1)	1.433(2)	1.441(1)	1.445(2)
S-C24	1.764(2)	1.754(2)	1.765(2)	1.770(2)
C1-C11-S	111.5(1)	110.9(1)	113.0(1)	111.8(1)
O1-S-O2	117.80(8)	117.6(1)	118.60(7)	118.42(9)
C11-S-C24	103.23(7)	103.2(1)	103.72(7)	106.67(8)
C1-C11-S-C24	176.3(1)	-178.6(1)	-55.3(1)	71.8(1)

^a Definitions: tilt stands for the dihedral angle of the least-squares planes of the cyclopentadienyl rings. The torsion angle C1-Cg2-Cg2-C6 reflects the mutual conformation of the substituents at the ferrocene unit; Cg1 and Cg2 are the centroids of the cyclopentadienyl rings C(1-5) and C(6-10), respectively.

Table 3. Selected distances and angles for **8a**, **8b**, and **9a** (in Å and deg.).^a

Parameter	8a (M/X = Na/Br)	8b (M/X = Na/I)	9a (M/X = K/Br)
Zn-P	2.4304(8)	2.445(1)	2.4310(6)
Zn-X1	2.3965(4)	2.6030(4)	2.4065(4)
Zn-X2	2.3980(4)	2.5956(4)	2.4049(4)
Zn-X3	2.4517(4)	2.6610(4)	2.4440(3)
M-X2	3.089(1)	3.362(2)	3.3218(6)
M-X3	3.010(1)	3.244(2)	3.2865(6)
M-O1	2.512(2)	2.485(3)	2.725(2)
M-O2 ⁱⁱⁱ	2.260(2) ⁱ	2.264(3) ⁱ	2.576(2) ⁱⁱⁱ
M-O1S	2.616(2)	2.686(3)	2.829(2)
M-O1S ^{ii/iv}	2.387(2) ⁱⁱ	2.399(3) ⁱⁱ	2.730(2) ^{iv}
Fe-C	2.024(3)-2.051(3)	2.034(3)-2.043(4)	2.027(2)-2.056(2)
tilt	4.1(2)	4.1(2)	5.1(1)
C1-Cg1-Cg2-C6	-85.6(2)	-84.7(2)	-85.4(1)
S-O1	1.446(2)	1.450(3)	1.444(2)
S-O2	1.439(2)	1.437(3)	1.442(2)

^a For definitions, see footnote to Table 2. Symmetry codes: *i.* 2-x, -y, -z; *ii.* 1-x, -y, -z; *iii.* 1-x, 1-y, -z; *iv.* -x, 1-y, -z.

Graphical Abstract Entry

Alkylation of 1'-(diphenylphosphino)-1-[(dimethylamino)methyl]ferrocene (**1**) with 1,3-propanesultone yields phosphinoferrrocene betaine **2**, which can be advantageously used as a ferrocenylmethylation agent in the synthesis of new phosphinoferrrocene ligands.

